ChemComm

Nickel(II) pincer complexes demonstrate that the remote substituent controls catalytic carbon dioxide reduction

Journal:	*ChemComm*
Manuscript ID	CC-COM-12-2017-009507.R2
Article Type:	Communication

Please do not adjust margins

Chem. Commun.

COMMUNICATION

Nickel(II) pincer complexes demonstrate that the remote substituent controls catalytic carbon dioxide reduction

Received 00th January 20xx,
Accepted 00th January 20xx

DOI: 10.1039/x0xx00000x

www.rsc.org/

Dalton B. Burks,[†,a] Shakeyia Davis,[†,b] Robert W. Lamb,[c] Xuan Liu,[d] Roberta R. Rodrigues,[b] Nalaka P. Liyanage,[b] Yujie Sun,[d] Charles Edwin Webster,*[,c] Jared H. Delcamp,*[,b] Elizabeth T. Papish,*[,a]

Abstract. The first example of a CNC pincer ligand with a central pyridinol ligand is reported in a nickel(II) complex. This metal complex can be protonated or deprotonated reversibly in situ to switch on or off the photocatalytic performance towards CO_2 reduction. The O^- substituent appears essential for catalysis.

Solar fuels via CO_2 reduction to form CO are potentially renewable and sustainable, if the problem of designing a robust and active catalyst can be overcome.[1] This work deals with the impact of changes in remote functional groups on catalyst activity. Specifically, we are investigating the role of protic π donors (OH groups) on the activity of nickel(II) complexes. Direct electrocatalytic reduction of CO_2 to $CO_2^{-\bullet}$ is an energetically demanding process (-1.99 V vs. SHE in H_2O at pH 7).[2] In practice, proton coupled electron transfer (PCET) can provide a lower energy pathway to CO formation ($CO_2 + 2e^- + 2H^+ \rightarrow CO + H_2O$ at -0.52 V vs. SHE in H_2O at pH 7). Importantly, PCET processes can be accelerated by having protic ligands near the metal center of the catalyst.[3] The catalyst also lowers the activation barrier for this reaction and can select for CO formation vs. other multi-electron products (HCO_2H at -0.61 V, HCHO at -0.49 V, CH_3OH at -0.38 V and CH_4 at -0.24 V vs SHE in H_2O at pH 7).[2, 4]

Chemists are still learning how to predict when a change in a remote substituent will greatly impact catalytic rates and catalyst longevity. This is especially true in the area of CO_2 reduction by both electrochemical and photochemical methods. Hydroxy (OH) groups (via covalently attached phenols) have been added to iron porphyrin-based catalysts and have resulted in improved turnover frequencies (TOFs) for electrocatalytic CO_2 reduction due to an increased local concentration of protons.[5] However, in the case of photocatalytic CO_2 reduction using these same phenol substituted iron complexes, these catalysts were prone to decomposition.[6] Similarly, a phenol group on the ligand is beneficial in electrocatalytic CO_2 reduction with a manganese(I) catalyst; again the OH group is thought to facilitate proton transfer and play a key mechanistic role.[7] In contrast, the use of the 4,4'- or 6,6'-dihydroxybipyridine (dhbp) ligand with Re(I) or Ru(II) complexes has illustrated that in this specific case, proximal hydroxyl groups are detrimental to electrocatalytic CO_2 reduction, and in fact the 6,6'-dhbp complexes only gives minimal activity (TON = 1 or less) with competing decomposition.[8, 9] Nonetheless, proximal OH groups (in bidentate[10] and tridentate[11] ligands) are generally beneficial in metal catalysts for the hydrogenation of CO_2[12-14] and other substrates. With these studies in mind, it was unclear at the outset of our work herein whether pyridinol derived pincers would enhance or reduce photodriven catalytic CO_2 reduction activity with nickel(II).

N-heterocyclic carbene (NHC) and pyridine rings have been combined to make bidentate, tridentate pincer, and tetradentate ligands for metal catalysts that are highly active for CO_2 reduction[15-19] and other reactions. Focusing on the group 10 metals,[20] tetradentate NCCN ligands bind to Ni(II) and form highly efficient photodriven catalysts for CO_2 reduction to CO.[15] Because pincer ligands often form highly active catalysts with earth-abundant metals, we aimed to affix a pyridinol-NHC pincer ligand to a Ni metal center. Thus, we can evaluate the effect of modulating electron density at the metal center with a π electron donor group (O^-) at the *para* (to N_{py}) position.[21] As shown below, this simple change converts inactive complexes to active photocatalytic systems.

Papish *et al*. recently reported a bidentate ligand that was the first to combine the NHC and pyridinol moieties, and these ligands supported Ir(III) and Ru(II) complexes that were studied for catalytic CO_2 hydrogenation.[12] However, thus far, no one has combined NHC and pyridinol derived rings on a pincer scaffold until our recent report that ruthenium complex **1**

[a] *University of Alabama (UA), Department of Chemistry, Shelby Hall, Tuscaloosa, AL 35487, USA. Email: etpapish@ua.edu.*
[b] *University of Mississippi, Department of Chemistry and Biochemistry, Coulter Hall, University, MS 38677, USA. Email: delcamp@olemiss.edu.*
[c] *Mississippi State University, Department of Chemistry, Hand Chemical Lab, Mississippi State, MS, 39762, USA. Email: ewebster@chemistry.msstate.edu.*
[d] *Utah State University, Department of Chemistry and Biochemistry, Widtsoe Hall, Logan, UT 84322, USA.*
† These authors contributed equally.
Electronic Supplementary Information (ESI) available: further experimental details and spectra including pK_a determinations. See DOI: 10.1039/x0xx00000x

This journal is © The Royal Society of Chemistry 20xx

Please do not adjust margins

(Figure 1) is an efficient catalyst for CO_2 reduction to CO. Complex **1** is a robust catalyst with selective formation of CO; in contrast complex **2**, with the unsubstituted pincer, is inactive. These recently reported results illustrate that a remote methoxy group can greatly enhance photocatalysis.[22] In this work, we aimed to use these new CNC pincer ligands with Ni(II), an earth abundant metal.

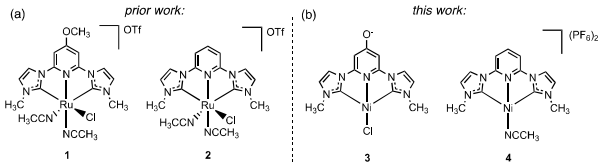

Figure 1: (a) Ru(II) photocatalysts (**1**: TON =250, **2**: TON = 3) for CO_2 reduction[22] and (b) Ni(II) complexes **3** and **4**.[23]

The synthesis of the nickel(II) complex **3** begins with the carbene precursor **L** (used here as the PF_6^- salt) which we recently reported (Scheme 1).[22] The synthesis of Ni(II) pincer complexes typically involves high heat (~160 °C) in several literature procedures.[24] Following these procedures, treatment of **L** with Ni(dme)Cl_2 in the presence of Na_2CO_3 as the base in DMSO resulted in loss of a methyl group to form the O^- substituted ligand in 29% yield (Scheme 1). It appears that high heat as well as excess free chloride resulted in methyl loss as methyl chloride, as our reaction conditions resemble known methods for deprotection of phenol derived ethers.[25] Complex **3** is neutral with Ni(II) ligated by a chloride and an anionic pincer. **3** was fully characterized by ^{1}H-NMR, IR, MS, and EA. The IR spectrum shows a peak at 1568 cm^{-1} which is consistent with C=O character. This complex has limited solubility in most solvents, but it can be studied in aprotic organic solvents like DMSO and CH_3CN. Complex **3** can be reversibly protonated to form cation **3A**. For example, in DMSO, triflic acid can protonate **3** and then proton sponge can be used to deprotonate **3A** as followed by UV-vis or ^{1}H-NMR spectroscopy (Figure S14 and S21, respectively). Acetic acid (pK_a = 12.3 in DMSO) appears to be too weak an acid to protonate **3**. These results show that the pK_a of **3A** is between zero and ~10 in DMSO. With the addition of sulfamic acid (pK_a = 6.5 in DMSO), an equilibrium between **3** and **3A** is reached as observed by UV-vis spectroscopy (Figure S13). This equilibrium constant was used to calculate the pK_a (**3A**) = 5.4(4) (*cf*. computationally we predicted a pK_a value of 3.9 in DMSO, see the ESI).

One could reasonably expect that a deprotonated oxygen would allow for a more electron-rich pyridyl ring, which could then donate more electron density to the metal center. Natural Atomic Orbital (NAO)[26] analysis was used to compare atomic charges between species. Upon deprotonation of **3A** to produce **3**, there is an increase in the negative charge on the O atom (+4%), the N_{py} atom (+5%), and the nickel atom (+2%), indicating that the protonation state does have an effect on the charge of the metal center. Along with the change in the atomic charges, the C-O distance decreases from 1.33 Å in **3A** to 1.25 Å in **3**. As expected with this decrease in bond length, the computed harmonic stretching frequency (ω_{CO}) shifts from 1513 cm^{-1} in **3A** to 1609 cm^{-1} in **3**, reflecting the increase in the carbonyl C-O bond order. Experimentally the C-O stretch shifts from 1448 cm^{-1} in **3A** to 1568 cm^{-1} in **3**. The changes in atomic charges and computed ω_{CO} are also reflected in deprotonation of the CNC-Ni fragment.

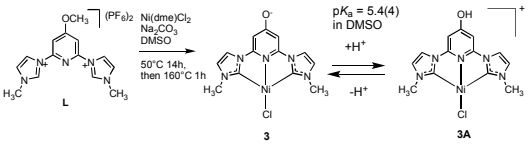

Scheme 1: Synthetic route to catalyst **3** and reversible protonation of **3** to give the acidic form, **3A**.

Complex **3** was evaluated for the electrocatalytic reduction of CO_2 via cyclic voltammetry (CV) experiments to compare with known electrocatalyst **4**.[23] Similar to catalyst **4**, a catalytic current increase was apparent for complex **3** at the third reduction wave (wave onset at -2.2 V vs Fc^+/Fc; i_{cat}/i_p = 6) when CV scans under argon and CO_2 atmospheres were compared (Figure 2). Upon addition of a proton source (H_2O) the current under CO_2 diminishes substantially, nearing the current observed at the third reduction wave under argon. This result suggests **3** is operating under a reductive disproportionation mechanism to give CO and CO_3^{2-} as the products (product analysis below) from CO_2.

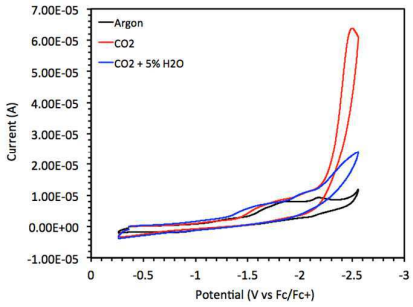

Figure 2. CVs of **3** under argon, CO_2, and CO_2 with added water. The electrolyte is 0.1 M Bu_4NPF_6 in CH_3CN with a glassy carbon working electrode, Ag/AgCl reference, and Pt counter electrodes. Each CV is a fresh solution of complex **3** (~0.1 mM, saturation limit).

Through the use of a photosensitizer (PS), nickel complexes are known to photocatalytically reduce CO_2.[15, 27, 28] Typically, the PS is first photoexcited to generate a reducing species, which accepts an electron from a sacrificial donor (SD, Figure S4). The reduced PS then can transfer an electron to the Ni catalyst, which may interact with CO_2 before accepting a second electron to reduce CO_2 to CO along with formation of H_2O or CO_3^{2-} (in the presence or absence of H^+, respectively).

Specifically, $Ir(ppy)_3$ [tris(2-phenylpyridine)iridium(III)] was selected as the PS due to its high photostability, reversible reduction and a potent reduction potential (-2.59 V vs. Fc^+/Fc, Figure 3).[19] 1,3-dimethyl-2-phenyl-2,3-dihydro-1H- benzo[d]-imidazole (BIH) was used as a SD because it is readily oxidized and is known to react with $Ir(ppy)_3$ during photolysis. We note

 This journal is © The Royal Society of Chemistry 20xx

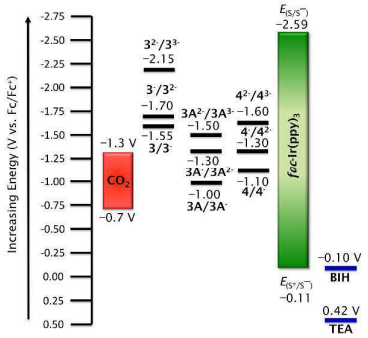

Figure 3: An energy level diagram with each catalyst, an estimated reduction potential range for CO_2, the PS, and each SD. Figure values are *estimated* from the onset of reduction waves as measured by CV (Fig. S5).

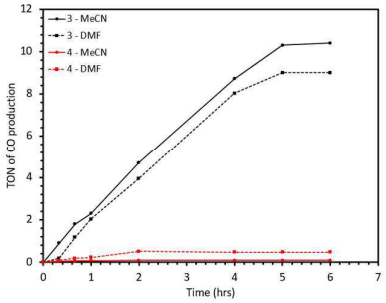

Figure 4. Turnover number versus time plot for photocatalytic reactions with complexes **3** and **4**.

that the $Ir(ppy)_3$/BIH system is energetically favourable for the transfer of an electron to the first three reduction potentials of **3**, **3A**, or **4** (Figure 3 and S5). However, there is a notable difference in driving force (550 mV) for electron transfer from complex **3** to CO_2 versus from complex **4** to CO_2 from the third catalyst reduction potential. In an acetonitrile solution with $Ir(ppy)_3$, BIH, and triethylamine (TEA) saturated with CO_2, complex **3** gives 10.6 turnovers (TON; moles CO/moles complex) when irradiated with a solar simulator to approximate natural sunlight over a six-hour period (Table 1, Figure 4). After 6 h of irradiation CO production ceases. Under identical conditions, complex **4** gives a TON of only 0.09. This difference in TON highlights the critical role of a remote O^- group in allowing for higher catalyst activity. Changing the solvent to DMF lead to a similar TON of 9.0 (Table 1, entry 3) for complex **3** and only 0.5 TON for complex **4**. When TEA was removed, the TON value for complex **3** dropped dramatically (Table 1, entry 5). TEA may serve multiple roles in the photocatalytic reduction of CO mixture (electron source, proton source after electron transfer, base). However, TEA is thermodynamically poorly positioned to serve as a SD (and thus as proton source) which suggests the primary role of TEA is as a base (Figure 3). Proton sponge is a surrogate base with a similar basicity to TEA (pK_a values are 9.00 and 7.50 in DMSO for the conjugate acids of TEA and proton sponge, respectively), but it has a dramatically higher energy oxidation potential of -0.15 V exceeding that of BIH (Figure S6). Reactions with proton sponge gave a TON of 5.6 with complex **3**, which suggests one of the primary roles of TEA is to serve as a base because the added electron donation strength of proton sponge did not improve the TON value (Table 1, entry 6). To test the effect of acid on photocatalysis with **3**, triflic acid (TfOH) was added as a strong acid and gave low reactivity (0.9 TON, Table 1, entry 7). This result highlights the importance of keeping the strongest acid in the solution at a relatively high pK_a value. The protonated complex **3A** is likely a poor catalyst due to the diminished electron donor strength from the OH group as evidenced through CV studies revealing **3A** is 550 mV lower in energy to reduce than **3** (Figure 3 and S5). Negative controls including the removal of $Ir(ppy)_3$, BIH, CO_2, or complex **3** produced <1 TON. Similarly, with **3** in the dark and all reaction components no CO is produced. Thus, all reaction components are needed and the observed CO is from photocatalytic CO_2 reduction. Additionally, the Hg-poison test suggests that the catalysis involves a homogeneous molecular species (Table S10).

Table 1. Photocatalytic CO_2 reduction under varied conditions.

entry	complex	change	TON_{max}
1	**3**	none	10.6
2	**4**	none	0.1
3	**3**	no MeCN, with DMF	9.0
4	**4**	no MeCN, with DMF	0.5
5	**3**	no TEA	1.8
6	**3**	no TEA, with proton-sponge	5.6
7	**3**	add TfOH, no TEA	0.9
8	**3**	no Ir	0.6
9	**3**	no BIH	0.3
10	**3**	no CO_2, with N_2	0.2

[a]Standard conditions: 0.1 mM Ni-complex, 0.1 mM $Ir(ppy)_3$, 11 mM BIH, 0.1 mL TEA, 1.9 mL MeCN, room temperature, and 150 W Xenon Lamp with an AM 1.5G filter for solar simulation.

The rate of reactivity of complex **3** was found to consistently give a turnover frequency (TOF; TON/time) of ~2.2 h^{-1} for the first 4 hours before CO production slowed at 5 hours and ceased by 6 hours (Figure 4). The difference in CO produced in MeCN versus DMF is largely due to ~30 additional minutes of sustained catalysis with MeCN as the initial rates over the first 4 hours are near identical. Providing the active catalyst results from dissociation of the Cl^- ligand on complex **3**, the similar rates in DMF and MeCN suggest this coordination site is not strongly associated with either solvent.

Computational studies (Figures 5, S28, S29, and S31-34) show that removal of chloride from $\mathbf{3A^0}$ produces fragment **5A** and from $\mathbf{3^-}$ produces fragment **5**. After deprotonation of **5A** to produce **5**, there is an increase in the negative charge on the O atom (+6%), the N_{py} atom (+6%), and the nickel atom (+6%). Furthermore, because coordination of CO_2 to the metal is a necessary step in catalysis, the relative energies of CO_2 binding to fragments **5A** (protonated) and **5** (deprotonated) were investigated (Figures S32 and S33). Starting with coordinatively unsaturated **5A**, attempts to locate a structure

with CO_2 coordinated to the nickel were unsuccessful. The resulting complex, **6A**, is a van der Waals complex (monopole/induced dipole) that has a Ni-C_{CO_2} distance of 3.32 Å and a nearly linear OCO bond angle (179.3°). In the case of the analogous deprotonated complex (**5**), the van der Waals complex exists (**6**); however, more importantly, a structure (**7**) with CO_2 bound to nickel can be located (Ni-C_{CO_2} = 2.04 Å). The charge of the CO_2 unit in complex **7**, which has bound CO_2, is –0.301. Furthermore, the charge of the CO_2 unit in complex **6A** (0.0074) is nearly zero (the sum of the NAO charges in free CO_2). These results suggest a plausible explanation for how protonation state influences the ability of the catalyst to reduce CO_2 to CO. Furthermore, the pincer ligand is less electron rich in complex **4** (cf. **3A** with OH) because it lacks an electron donor group, which may explain the photocatalytic inactivity. Via CV studies it is clear that the reduction potential of **3A** is dramatically shifted more positive from that of **3** (Figures 3 & S5). In contrast **3** (O^- group) is active with greater electron density supplied from the pincer to Ni.

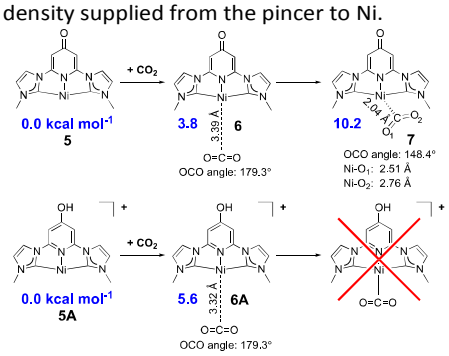

Figure 5. Computational study of CO_2 reduction from two different protonation states. Relative energies are in blue.

In summary, a surprising effect from a single remote atom change from a hydrogen (in **4**) to an oxygen anion (in **3**) on the pincer CNC ligand resulted in a dramatic increase in catalyst reactivity, effectively turning on CO_2 reduction. Complex **3** may be a pre-catalyst based on initial complex **3** showing catalytic current on the third reduction wave initially before a species with catalytic activity on the first reduction wave grows in. Sustained photocatalytic reactivity was observed for complex **3** in the presence of a photosensitizer for the first 6 hours. This study highlights the importance of careful remote substituent selection as a single atom substitution on a ligand can render an active complex completely inactive. Furthermore, these are switchable catalysts that can be "turned off" or "turned on" by manipulating the concentration of protons in solution.

We gratefully acknowledge financial support from the US National Science Foundation (OIA-1539035 to CEW, JHD, and ETP), a GAANN fellowship to DBB (P200A150329), and UA.

Conflicts of Interest

We have a patent pending on content related to this manuscript.

Notes and references

1. M. Robert, *ACS Energy Lett.*, 2016, **1**, 281-282.
2. Y. Matsubara, D. C. Grills and Y. Kuwahara, *ACS Catal.*, 2015, **5**, 6440-6452.
3. T. Zhang, C. Wang, S. Liu, J.-L. Wang and W. Lin, *J. Am. Chem. Soc.*, 2014, **136**, 273-281.
4. E. E. Benson, C. P. Kubiak, A. J. Sathrum and J. M. Smieja, *Chem. Soc. Rev.*, 2009, **38**, 89-99.
5. C. Costentin, M. Robert and J.-M. Savéant, *Acc. Chem. Res.*, 2015, **48**, 2996-3006.
6. J. Bonin, M. Chaussemier, M. Robert and M. Routier, *ChemCatChem*, 2014, **6**, 3200-3207.
7. J. Agarwal, T. W. Shaw, I. Schaefer, Henry F and A. B. Bocarsly, *Inorg. Chem.*, 2015, **54**, 5285-5294.
8. L. Duan, G. F. Manbeck, M. Kowalczyk, D. J. Szalda, J. T. Muckerman, Y. Himeda and E. Fujita, *Inorg. Chem.*, 2016, **55**, 4582-4594.
9. G. F. Manbeck, J. T. Muckerman, D. J. Szalda, Y. Himeda and E. Fujita, *J. Phys. Chem. B.*, 2015, **119**, 7457-7466.
10. I. Nieto, M. S. Livings, J. B. Sacci, L. E. Reuther, M. Zeller and E. T. Papish, *Organometallics*, 2011, **30**, 6339-6342.
11. C. M. Moore, B. Bark and N. K. Szymczak, *ACS Catal.*, 2016, **6**, 1981-1990.
12. S. Siek, D. B. Burks, D. L. Gerlach, G. Liang, J. M. Tesh, C. R. Thompson, F. Qu, J. E. Shankwitz, R. M. Vasquez, N. S. Chambers, G. J. Szulczewski, D. B. Grotjahn, C. E. Webster and E. T. Papish, *Organometallics*, 2017, **36**, 1091-1106.
13. W.-H. Wang, J. F. Hull, J. T. Muckerman, E. Fujita and Y. Himeda, *Energy Environ. Sci.*, 2012, **5**, 7923-7926.
14. J. F. Hull, Y. Himeda, W.-H. Wang, B. Hashiguchi, R. Periana, D. J. Szalda, J. T. Muckerman and E. Fujita, *Nature Chem.*, 2012, **4**, 383-388.
15. V. S. Thoi, N. Kornienko, C. G. Margarit, P. Yang and C. J. Chang, *J. Am. Chem. Soc.*, 2013, **135**, 14413-14424.
16. V. S. Thoi and C. J. Chang, *Chem. Commun.*, 2011, **47**, 6578.
17. J. Agarwal, T. W. Shaw, I. Stanton, Charles J, G. F. Majetich, A. B. Bocarsly and I. Schaefer, Henry F, *Angew. Chem. Int. Ed.*, 2014, **53**, 5152-5155.
18. N. P. Liyanage, H. A. Dulaney, A. J. Huckaba, J. W. Jurss and J. H. Delcamp, *Inorg. Chem.*, 2016, **55**, 6085-6094.
19. A. J. Huckaba, E. A. Sharpe and J. H. Delcamp, *Inorg. Chem.*, 2016, **55**, 682.
20. J. A. Therrien, M. O. Wolf and B. O. Patrick, *Inorg. Chem.*, 2015, **54**, 11721-11732.
21. A. A. Danopoulos, D. Pugh, H. Smith and J. Saßmannshausen, *Chem. Eur. J.*, 2009, **15**, 5491-5502.
22. C. M. Boudreaux, N. P. Liyanage, H. Shirley, S. Siek, D. L. Gerlach, F. Qu, J. H. Delcamp and E. T. Papish, *Chem. Commun.*, 2017, **53**, 11217-11220.
23. M. Sheng, N. Jiang, S. Gustafson, B. You, D. H. Ess and Y. Sun, *Dalton Trans.*, 2015, **44**, 16247-16250.
24. K. Inamoto, J.-i. Kuroda, K. Hiroya, Y. Noda, M. Watanabe and T. Sakamoto, *Organometallics*, 2006, **25**, 3095-3098.
25. K. Jarowicki and P. Kocieński, *Journal of the Chemical Society, Perkin Transactions 1*, 1999, **0**, 1589-1616.
26. A. E. Reed, R. B. Weinstock and F. Weinhold, *J. Chem. Phys.*, 1985, **83**, 735-746.
27. M. F. Kuehnel, K. L. Orchard, K. E. Dalle and E. Reisner, *J. Am. Chem. Soc.*, 2017, **139**, 7217-7223.
28. D. Hong, Y. Tsukakoshi, H. Kotani, T. Ishizuka and T. Kojima, *J. Am. Chem. Soc.*, 2017, **139**, 6538-6541.

This journal is © The Royal Society of Chemistry 20xx
Please do not adjust margins

Please do not adjust margins

This journal is © The Royal Society of Chemistry 20xx

Please do not adjust margins

TOC Graphic

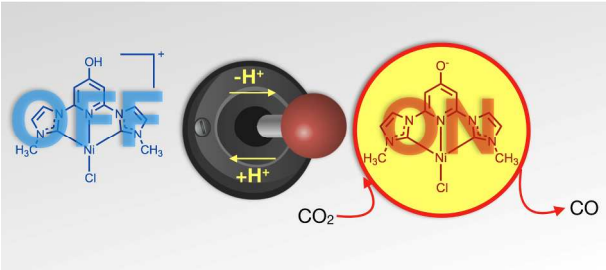

- **Synopsis:** New pincers containing a pyridinol ring form active nickel catalysts for CO_2 reduction, and interestingly protonation switches the catalyst off.